Journal of Mathematical Sciences and Modelling, 5 (2) (2022) 67-79
Review Article

Journal of Mathematical Sciences and Modelling

Journal Homepage: www.dergipark.gov.tr/jmsm
ISSN 2636-8692
DOI: http://dx.doi.org/10.33187/jmsm.1126076

Mathematical Modeling Application in Energy Conversion and Energy Storage

Nagihan Delibaş[1*], Seyyed Reza Hosseini[2] and Aligholi Niaei[1,2]

[1]*Department of Physics, Faculty of Science, University of Sakarya, Sakarya, Turkey*
[2]*Department of Chemical Engineering, University of Tabriz, 5166616471 Tabriz, Iran*
[*]*Corresponding author: caylak@sakarya.edu.tr*

Article Info

Keywords: *Battery, Fuel cell, Mathematical modeling, Simulation, Solar cell, Supercapacitor*
2010 AMS: *97M10, 97M50, 97N60*
Received: *4 June 20222*
Accepted: *10 August 2022*
Available online: *30 August 2022*

Abstract

The use of mathematical modeling to predict and investigate the effect of process variables in the research and engineering field of energy conversion and energy storage has also received special attention from scientists and industrial designers in this field due to their importance in the global economy. This review article investigates the applications of mathematical modeling and simulation in energy conversion and energy storage processes, and finally, with a case study, the application of mathematical modeling in the desired processes to be tested and compared with the reported results in the papers. In the first part, the main emphasis is on energy conversion, especially on the structure of solar cells and fuel cells and mathematical modeling methods, and predicting the effect of operating variables on their performance. The basic principles of modeling solar cells and fuel cells to understand the relationships governing the current, voltage, performance, and power of PV modules are to be discussed. And with a case study, modeling of the process to estimate the performance of PV modules and SOFC in various conditions has been investigated. In the second part, the main focus is on the mathematical modeling of energy storage devices including batteries and supercapacitors. Supercapacitors and batteries are electrochemical energy storage devices that can be charged within a few seconds to a few minutes. This efficient energy storage is based on the electrocatalytic effect of the electrode with a high surface area. The mathematical equations governing the battery and supercapacitor are discussed in the article, and battery and supercapacitor performance are to be simulated as a case study. Due to the Multiphysics nature of energy conversion and storage systems, the simulation is performed in two stages. In the first step, the semiconductor equations are applied and the electrical response of the electrochemical device is modeled. In the second step, if needed, the thermal equations can be entered into the main calculations and the net amount of heat and the temperature profile in the desired device is evaluated. The main goals and ideas of compiling this review article are expressing the importance and role of electrochemical and electrocatalysts in energy production and storage processes and paying attention to the governing mechanism and mathematical equations and highlighting important and common models used in different parts of energy conversion and storage in a coherent article.

1. Introduction

1.1. Why do mathematical modeling?

Mathematical modeling has always been an important activity in all scientific research and development in science and engineering. On another side, the model formulation of qualitative questions and physical phenomena, as mathematical problems was an important motivation

Email addresses and ORCID numbers: caylak@sakarya.edu.tr, 0000-0001-5752-062X (N. Delibaş), sr.hosseini.sr@gmail.com, 0000-0002-0946-7489 (S. R. Hosseini),) aniaei@tabrizu.ac.ir, 0000-0001-5580-4266 (A. Niaei)

for and an integral part of the development of mathematics from the very beginning. In the last decades, the use of mathematics as a very effective tool in problem-solving has gained prominence, mainly due to rapid developments in computing. Computational calculations are particularly important in modeling chemical engineering processes because of the complexity of the physical and chemical laws of these processes. In the chemical processes, heat and mass balances and also momentum balances, are basic mathematical models used in the modeling of chemical reactions engineering. Nevertheless, mathematical equations are the best tools for engineers and scientists to understand important systems and processes. In all engineering contexts, mathematical modeling is a prerequisite such as process control, optimization, mechanistic understanding, design and planning of experiments, simulation instead of costly experiments, feasibility studies, and scale-up of the process.

This article reviews mathematical modeling applications in energy conversion and energy storage. So, it focuses on the energy sector in two sections. In the first section, the major emphasis is on energy conversion, especially on solar cells and fuel cells' structure and methods of modeling and predicting their performances. In the second section, the major emphasis is on energy storage focuses on modeling the structure and performance of batteries and supercapacitors. Supercapacitors and batteries are electrochemical energy storage devices that can be charged in a matter of seconds to minutes. This efficient energy storage is based on an electrolyte's adsorption to a high-surface-area electrode. These marvelous properties led to extensive concerted research into the nature of the storage mechanism, electrode design, and especially new optimized materials. Because of the multi-physics nature of energy conversion and storage systems, the simulation is performed in two steps. In the first step, the semiconductor equations are applied and the electrical response of the electrochemical device is modeled. The second step calculates the thermal equations, while the heat generated in the first step is used as the heat source.

2. Energy Conversion in Solar Cells and Fuel Cells

2.1. Solar Cells

Solar energy is one of the applicable substitutions for non-renewable energy generation sources. Devices that are utilized for solar energy applications are named solar panels which are consisted of solar cells on small scales. These devices are a subset of photovoltaic systems. Their performance is based on two charge carriers named electron with negative charge and hole with positive charge. These opposite charges lead to potential differences through electrodes and accordingly electricity generation. In the practical phase, solar cells are synthesized and deposited in laboratories. Besides, solar panels are fabricated for industrial applications. However, a better understanding of photovoltaic devices' design, simulation, and modeling application are required. It will help researchers to reduce experimental and fabrication errors.

In the case of solar cell simulation, many numerical and modeling software packages were developed. Among them, SCAPS-1D and COMSOL-Multiphysics simulators are common [1, 2]. All of the software packages employ three basic equations including Poisson and electron and hole continuity equations in their software base. In a general perspective, solar cell simulation is performed in three physics containing electrical, optical, and thermal considerations. The base of modeling in the mentioned physics is as below:

2.1.1. Optical section modeling

All of the software packages utilize some basic optical assumptions. Among them, the most popular ones refer to air mass and reflection in the electrodes. Air mass is relevant to the sun's angle with the PV system. In most simulations, the 48° angle or A.M.1.5 is assumed. The other important factor in the optical part refers to the reflection in the front electrode that can be designed in some software packages [3].

2.1.2. Electrical section modeling

In the second physics named electrical part, the Poisson equation (2.1) and the continuity equations for electrons (2.2) and holes (2.3) are solved simultaneously [4, 5]:

Poisson's equation:

$$\nabla.\varepsilon\nabla\phi = -q(p-n+N_D-N_A) \tag{2.1}$$

Electron continuity equation:

$$\frac{\partial n}{\partial t} = \frac{1}{q}\nabla j_n + G_n - U_n \tag{2.2}$$

Hole continuity equation:

$$\frac{\partial p}{\partial t} = \frac{1}{q}\nabla j_p + G_P - U_P \tag{2.3}$$

U_n and U_p are the electron and hole recombination rates, respectively. It should be noted that the recombination factor refers to the dissipation created due to the electron and hole recombination. G_n and $G_p$are the total rate of electron and hole generation, respectively.

One of the parameters required for the calculations of this part is the refractive index and the extinction coefficient related to each layer of the solar cell, which must be considered [6]-[10]:

$$G(y) = \int_{280nm}^{4000nm} -a(\lambda)\,\phi(y,\lambda)\,d\lambda$$

Three types of recombination may occur in solar cells: radiative recombination, SRH (Shockley Reed Hall) recombination, and Auger recombination. Note that the SRH recombination is enabled in the semiconductor module:

$$R_{SRH} = \frac{np - {n_j}^2}{\tau_n \left(n + n_j \exp\left(-\frac{E_T - E_j}{K_B T}\right)\right) + \tau_p \left(p + n_j \exp\left(-\frac{E_T - E_j}{K_B T}\right)\right)}$$

2.1.3. Thermal section modeling

This modeling is set in a few software packages. For instance, the COMSOL software is capable of considering thermal physics in solar cell simulation. The physics of heat transfer in solids for thermal calculations is used. The equation (2.4) governing heat transfer is as follows:

$$-k\nabla^2 T + Q = \rho_p C_p \frac{dT}{dt} \tag{2.4}$$

Where k is the conductive heat transfer coefficient of the material $[W/m.K]$, C_P is the specific heat $[J/(kg.K)]$, ρ is the density $\left[kg/m^3\right]$. Q is the term for heat generation due to various factors. *A* summary of each model was mentioned in the previous sections. They are the basics of the physics of each simulation software.

2.1.4. Case studies

As mentioned above, some of the results of recent studies around the applications of solar cells simulation and modeling tools in some custom solar cells are given.

In 2021, Hosseini et al. [2] studied the effect of different layer properties of a perovskite solar cell such as their thickness and charge carrier density and obtained their optimal parameters using SCAPS-1D software. The optimum cell's final current-voltage curve was represented in Figure 2.1 Another simulation study with the SCAPS-1D tool was performed by Hosseini et al. in 2021 that was based on investigating different configurations of HTL in a custom perovskite solar cell, [11]. They studied three common HTL types, Spiro-OMeTAD, P_3HT, and Cu_2O, and their effects on cell performance in different composite, tandem, and single forms, and their results were compared.

Moreover, other simulation tools were employed by researchers in recent years. For instance, Delibas et al. [1], investigated the effect of using different hole transfer layers, both polymeric and non-polymeric by using COMSOL Multiphysics software. For this purpose, three HTM layers (Spiro-OMETAD, $CuSCN$, P_3HT) have been investigated. The I-V curves of the mentioned structures were collected in Figure 2.1.

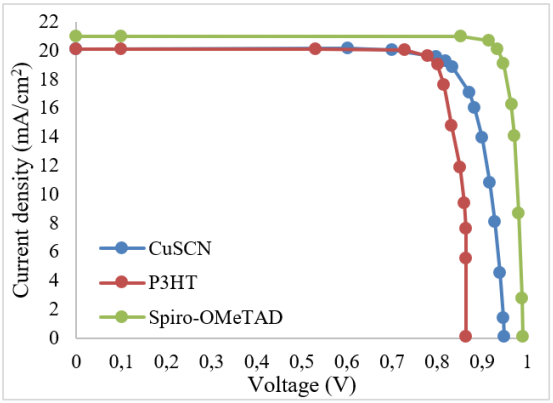

Figure 2.1: Current-Voltage Curve of the Perovskite Solar Cell using different HTMs [1]

A summary of the mentioned studies' performance parameters (electrical-optical physics) was given in Table 2.1.

It should be noted that the parameters mentioned in Table 2.1 including VOC, JSC, FF, and PCE refer to the solar cell's open circuit voltage, short circuit current, Fill Factor, and power conversion efficiency, respectively.

All of the studies mentioned in Table 2.1, were validated with similar experimental data. For instance, according to the data validated for the Au/ Spiro-OMeTAD/ $CH_3NH_3PbI_3$/ TiO_2/ FTO in the mentioned work in the table ([11]), the photovoltaic parameters including V_{OC}, J_{SC}, FF, PCE was $1.08V$, $22.43\ mA/cm^2$, 79.63%, 19.26% for simulation and $0.98V$, $21.20 mA/cm^2$, 77.60%, 18.70% for experimental works, respectively.

In 2021, Bouarissa et al. modeled a CZTS solar cell with the new proposed $ZnO/MoS_2/CZTS$ structure using the SCAPS-1D software package. They performed the optimization of each layer's thickness and obtained a final efficiency of about 23% [12]. In another study, in 2021, Islam et al. studied the numerical modeling of a $CdTe$ solar cell with the WS_2 buffer layer through SCAPS-1D simulation. They obtained an efficiency of 20.55 % [13].

Other simulation tools were employed to perform the numerical modeling of solar cells. In 2021, microcrystalline silicon solar cells were simulated by Plotnikova et al. using TCAD software. In that research, the structures and characteristics of the custom solar cell were

Configuration	Structure	V_{OC} (V)	J_{SC} (mA/cm^2)	FF (%)	PCE (%)	Ref.
simple	Au/ Spiro-OMeTAD/ P_3HT/ $CH_3NH_3PbI_3$/ TiO_2/ FTO with the ultrathin P_3HT polymeric layer	1.18	25.54	88.11	26.52	[2]
simple	Spiro-OMeTAD	1.08	22.43	79.63	19.26	[11]
	P_3HT	0.87	32.09	57.09	15.92	[11]
	Cu_2O	1.08	22.44	81.60	19.77	[11]
composite	$(Spiro\text{-}OMeTAD)_{0.1}(P_3HT)_{0.9}$	1.05	29.59	79.37	24.57	[11]
	$(Spiro\text{-}OMeTAD)0(Cu_2O)1$	1.08	22.44	81.60	19.77	[11]
	$(Cu_2O)_{0.4}(P_3HT)_{0.6}$	1.02	25.00	80.84	20.66	[11]
tandem	$Spiro\text{-}OMeTAD/P_3HT$	1.09	31.47	78.37	26.97	[11]
	$P_3HT/Spiro\text{-}OMeTAD$	1.08	22.43	77.86	18.81	[11]
	$Spiro\text{-}OMeTAD/Cu_2O$	1.08	22.44	81.03	19.63	[11]
simple	Spiro-OMeTAD	21	0.973	82.00	16.80	[1]
	CuSCN	20	0.949	83.00	15.70	[1]
	P_3HT	20	0.720	84.00	12.10	[1]

Table 2.1: The photovoltaic parameters obtained for different perovskite solar cells studies [2].

obtained and the photovoltaic parameters were calculated using the TCAD modeling system [14]. For other modeling tools, a simulation was performed in 2020 by Rasheed et al. using MATLAB software. The simulation was performed around Single-Diode solar cells. In their study, they suggest and analyze two algorithms; a new Inverse Quadratic Interpolation and Illinois for solving the nonlinear equation of a solar cell single diode type with initial value $x0$ and load resistance R varies from 1 to 5 Ω is implemented in MATLAB program. Using five numerical testes examples, the results secured reveal that the suggested algorithm has lesser iterations than the other method (Illinois method), so the accuracy and efficiency of the proposed method are the best [15].

In the case of thermal modeling, in 2019, Saxena et al. [16] presented an extended 3D simulation of heat distribution in perovskite solar cells. They studied the temperature distribution in conventional perovskite solar cells through paired optical-electrical-thermal modules. The wave optical module, the semiconductor module, and the heat transfer in the solid module are coupled in their simulation in the 3-D wizard. The simulation results indicated that the heat generated in the cell is best dissipated from the metallic contact where the $PbI2$ defect forms because of oxidation or decomposition of the perovskite layer at moisture exposure.

In conclusion, it can declaim that simulation can possess many positive effects in understanding the behaviors of solar cells and can help us orientation in solar cell study.

2.2. Fuel cells: Current, temperature, and concentration distribution of a solid oxide fuel cell with COMSOL: 3D modeling

2.2.1. Why is solid oxide fuel cell?

Solid Oxide Fuel Cell (SOFC) is one of the important parts of energy conversion systems. The most significant parts of SOFC are two electrodes and the electrolyte between them. Anode and cathode electrodes should be porous, ion conductor, electron conductor, thermally compatible with electrolytes, and stable in high temperatures. For a good understanding, Figure 2.2 demonstrates the operation of $SOFC$ with H_2 as fuel [17]-[19].

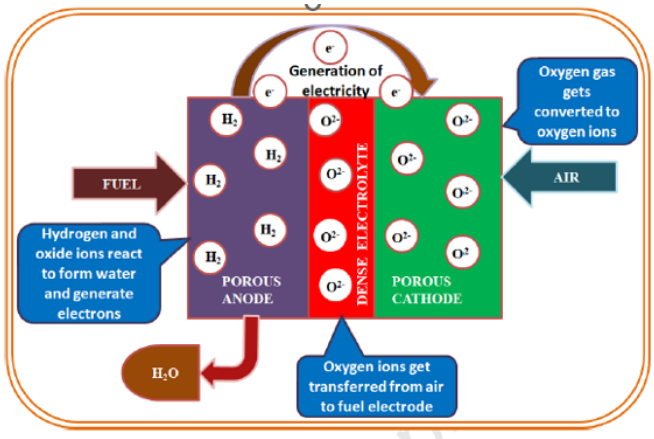

Figure 2.2: The operation of SOFC with H2 as fuel [19].

The main structure of SOFC, which contains the electrolyte has some special properties like being dense, ion conductor, thermally compatible with electrodes, stable in both reduction and oxidation environments, and weak electron conductor or not being an electron conductor at

all. In the cathode, the oxygen reduction reaction (ORR) happens, and then the oxygen transfers to the anode through the electrolyte and anode, where the hydrogen turns to the proton, oxygen ions and protons react and turn to water. Generally, the following mechanisms can be described these phenomena:

$$\frac{1}{2}O_2 + 2e^- \rightarrow O^{2-}$$

$$O^{2-} + H_2 \rightarrow H_2O + 2e^-$$

In this reaction, electrons are released and transferred to the cathode and this way electricity required for transport, or electronic devices can be produced [20]-[23].

2.2.2. Mathematical modeling in SOFC

To simulate SOFC in 3D, to be used the capabilities of COMSOL Multiphysics software to draw models in 2D. At first, a cross-section of the desired SOFC is to be drawn in the work plane, then with the use of Extrude mode, turn the two-dimensional model into a three-dimensional model (Figure 2.3).

In this modeling, the secondary current distribution, gas diffusion in porous media and flow channels, transport of concentrated species, and heat transfer in solids and fluids are considered. The detail of this mentioned section is described in detail below (2.5)-(2.7):

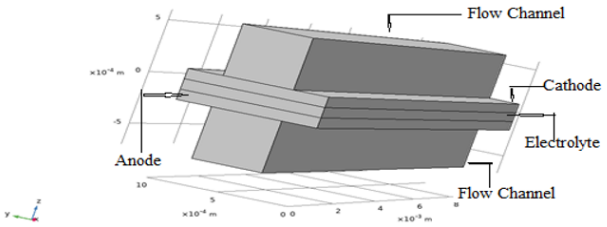

Figure 2.3: Two-dimensional model into a three-dimensional model [18].

Secondary Current Distribution: The relationship between charge transfer and over potential can be described using the Butler-Volmer and Tafel equations as below:

$$i = i_{o.a}\left[\frac{C_{h_2}}{C_{h_{2.ref}}}\exp\left(\frac{0.5F\eta}{RT}\right) - \left(\frac{C_{h_{2o}}}{C_{h_{2.ref}}}\right)\exp\left(\frac{-1.5F\eta}{RT}\right)\right] \tag{2.5}$$

where $i_{o.a}$, F, C_{h2}, C_{h2o} the are the anode exchange current density, the Faraday's constant, molar concentration of H_2 and the molar concentration of H_2O respectively.

The overvoltage is defined by:

$$\eta = \phi_{electronic} - \phi_{ionic} - \Delta\phi_{eq} \tag{2.6}$$

where $\Delta\phi_{eq}$ is the equilibrium potential difference. The cathode charge transfer kinetics is given by:

$$i = i_{0.c}\left[\exp\left(\frac{3.5F\eta}{RT}\right) - x_{o2}\left(\frac{C_t}{C_{o2.ref}}\right)\exp\left(\frac{-0.5F\eta}{RT}\right)\right] \tag{2.7}$$

where $i_{0.c}$ is the cathode exchange current density and $x_{o2}$is the molar fraction of O_2.

Gas diffusion in porous media and flow channel: For gas diffusion in porous electrodes calculation, the Brinkman equation (2.8) is used:

$$\nabla p = -\frac{\mu}{K}v + \mu_e\nabla^2(v) \tag{2.8}$$

where v, μ, and μ_e is the fluid velocity, fluid viscosity, and effective viscosity parameter respectively.

And the weakly compressible Navier-Stokes equation (2.9) is used for modeling gas flows in open channels:

$$\rho\left(\frac{\partial u}{\partial t} + u.\nabla u\right) = -\nabla p + \nabla\left(\mu\left(\nabla u\right) + \left(\nabla u\right)T\right) - \frac{2}{3}\mu\left(\nabla u\right)I) + F \tag{2.9}$$

where u, p, ρ, μ and F are the fluid velocity, fluid pressure, fluid density fluid dynamic viscosity, and external forces respectively [21]-[23].

Transport of concentrated species: The Stefan- Maxwell equation (2.10) is used to modeling of fluid transfer, both bulk transfer and diffusion in porous electrodes (anode and cathode flow channels).

$$\frac{\partial \rho \omega_i}{\partial t} + \nabla.(j_i + \rho \omega_i u) = R_i \tag{2.10}$$

where $\rho\omega_i$, j_i, and R_i denotes the density, the mass fraction molecular mass flux, and reaction rate respectively.

Heat transfer in solids and fluids: The general equation (2.11) of heat transfer intended for the model is given below. In this model, it is used steady state heat transfer and considered the convection heat transfer only for gas channels. In addition, it is ignored radiation heat transfer.

$$\rho.c_p.u.\nabla T = \nabla.(k\nabla T) + Q \tag{2.11}$$

Here Q is the heat generation or consumption, k is the effective thermal conductivity, T is the temperature, and cp is the gas phase-specific heat. The heat generated by electrochemical suction, ohmic polarization, etc. given by (2.12):

$$Q = i.\left(\frac{T.\Delta S_r}{n_e.F} + \eta\right) + \sum \frac{i^2}{\sigma} + \sum \left(r_{ref}.\Delta H_{ref}\right) \tag{2.12}$$

where ΔS_r is the entropy change of the reaction, r_{ref} the reforming reaction rates $\left(in\,mol/m^3 s\right)$, and ΔH_{ref} the enthalpy of the reactions.

The energy equation (2.13) for the anode and cathode channel walls is as follows:

$$n.(-k\nabla T) = h.\left(T_w - T_f\right) \tag{2.13}$$

where T_w is the channel wall temperature and T_f is the fluid temperature and h is the heat transfer coefficient in gas flow channels is calculated by the Nusselt number [24]-[26].

2.2.3. Numerical simulation

Based on the geometry and physics of the problem shown in Figure 2.5, after selecting the appropriate boundary conditions, the fuel cell mesh is adjusted and the model is prepared with mathematical equations that can be solved numerically by the FEM method in COMSOL or any similar software's. It is noteworthy that to increase the accuracy of calculations, the meshing in the electrode and electrolyte sections is finer compared to flow channels.

2.2.4. Case study

To apply the governing mathematical equations in the fuel cell, a sample cell study with certain characteristics has been simulated in the COMSOL environment. In this study, a three-dimensional mathematical model of a SOFC that can show the temperature, concentration, and distribution of current inside the cell and the performance of a solid oxide fuel cell is investigated and analyzed. In addition, the flow pattern parameter and operational variables such as input and output current affect the cell performance. The flow pattern changes from the opposite flow to the simultaneous flow. The results showed that the temperature distribution, flow, and concentration of reactants (O_2 and H_2) are related and wherever the concentration of substances is higher, cell performance and the amount of temperature and flow produced increase. However, solid oxide fuel cell performance is better when the flow pattern is concurrent. The results of the study when the flow pattern was simultaneous, both the cathode and anode currents entered from behind the fuel cell and exited the front of the cell.

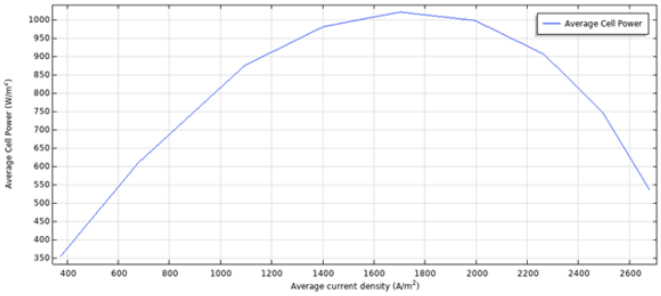

Figure 2.4: Power density- current density plot for counter-current flow pattern [18].

For the reverse flow pattern, the input of the cathode current channel is behind the cell while the input of the anode current channel is in front of the fuel cell. The results of this study in Figures 2.4 and 2.5 show a three-dimensional view of the temperature distribution across the fuel cell [18].

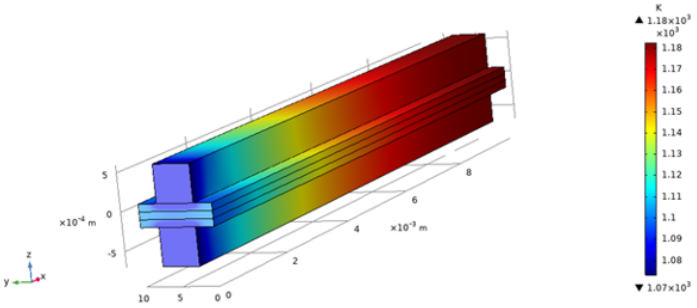

Figure 2.5: Distribution of temperature inside the cell for co-current flow pattern [18].

3. Energy Storage in Batteries and Supercapacitors

3.1. Batteries

The energy stored in the batteries is very important in the energy sector and can be used to power your home and help stabilize the grid. Therefore, batteries are one of the important technology platforms that can be used to improve the state of the world and combat climate change. Electric vehicle battery could be used to help power homes and stabilize the grid. Batteries will increasingly play important role in the future world. different materials in the structure of batteries have different electrochemical properties, and so they produce different results when you put them together in a battery cell. So, in this study, it focused on one of the important batteries with a Lithium-ion structure [27]-[30]. Lithium-ion batteries are an important source of energy storage that attracts scientists and researchers to improve their performance experimentally and computationally. The schematic structure of an electrochemical cell of a lithium-ion (Li-ion) battery is shown in the Figure 3.1. Computational work can help researchers predict and optimize battery performance, saving time and money. The use of mathematical modeling along with powerful simulations such as COMSOL is a great help in designing and creating new ideas in this field. By modeling and simulating different batteries with different geometries and structural materials are designed and their performance is tested in different conditions. High-efficiency batteries are designed by analyzing the results obtained from mathematical modeling and simulation. In this study, the simulation of the discharge mode of the battery connected to the consumer with constant current density is investigated. As a study sample, COMSOL simulation software was performed [31, 32].

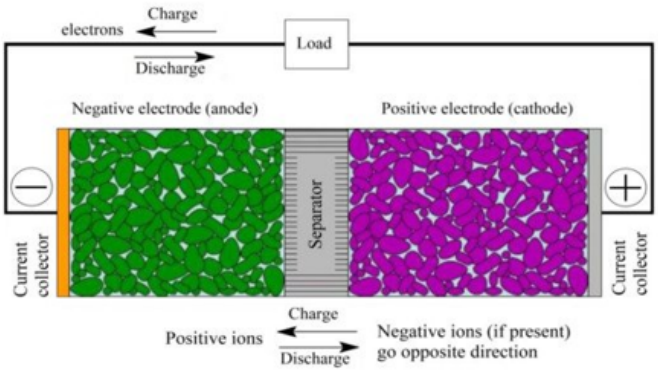

Figure 3.1: The detailed structure of an electrochemical cell of a lithium-ion (Li-ion) battery [28].

3.2. Mathematical models

A simplified structure of a Lithium-ion battery, with the geometry as shown in Figure 3.2 was used and the mathematical model was used based on this two-dimensional structure [33, 34].

The battery in this simulation consists of a negative electrode, an electrolyte, and a positive electrode, in which the negative electrode is applied to the geometry in the form of a surface boundary condition, but the electrolyte and the positive electrode are applied to the geometry of the software. The general module for solving this simulation is a Lithium-ion battery. The main important and relevant equations (3.1)-(3.4) that be used in the COMSOL software are demonstrated below [35]-[37].

$$\frac{\partial c}{\partial t} + \nabla . J_1 = R_1 \tag{3.1}$$

$$\frac{\partial c}{\partial t} + \nabla . J_1 = R_1 \tag{3.2}$$

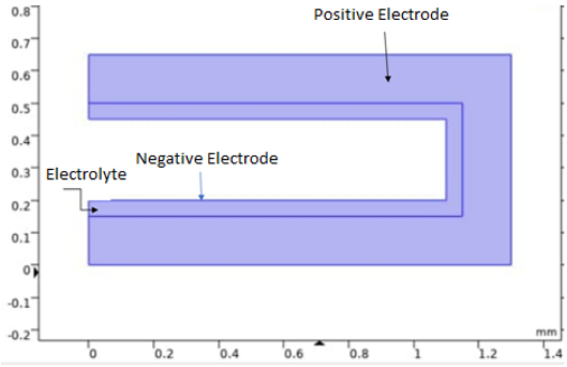

Figure 3.2: Two-dimensional simulation of a Li-ion battery [27].

$$J_1 = -D_1 \nabla c_1 + \frac{i_1 t_+}{F} \tag{3.3}$$

$$i_1 = \sigma_1 \nabla \phi_1 + \frac{2\sigma RT}{F}\left(1 + \frac{\partial \ln f}{\partial \ln c_1}\right)(1 - t_+)\nabla \ln c_1 \tag{3.4}$$

For the electrode and electrolyte, the "Electrode Surface" the suitable boundary condition was used in the COMSOL software. For the electrolyte, $LiPF_6$ has been used, the parameters of which are available in the software database. For the positive electrode, $LiMn_2O_4$ has been used, and the parameters required to simulate this material are also available in the database of COMSOL software. For the Positive electrode, the Porous Electrode boundary condition is added to the volume of the positive electrode in the simulation geometry. As the name implies, in this case, the electrode is considered a porous space and the fine particles penetrate the porous spaces which are considered spherical. The equations (3.5)-(3.12) used in this boundary condition are shown below:

$$\nabla . J_\iota = R_1, R_1 = -\sum_m \frac{v_{Li+,m}\, i_{v,m}}{F} + R_{l,src} \tag{3.5}$$

$$\nabla . i_l = i_{v,total} + Q_l \tag{3.6}$$

$$\nabla . i_s = i_{v,total} + Q_s \tag{3.7}$$

$$J_1 = -D_{l,eff} \nabla c_1 + \frac{i_l t_+}{F} \tag{3.8}$$

$$i_l = -\sigma_{,eff} \nabla \phi_l + \left(\frac{2\sigma_{l,eff} RT}{F}\right)\left(1 + \frac{\partial \ln f}{\partial \ln c_l}\right)(1 - t_+)\nabla \ln c_l \tag{3.9}$$

$$i_s = -\sigma_{s,eff} \nabla \phi_s \tag{3.10}$$

$$D_{l,eff} = {\varepsilon_l}^{1.5} D_l, \sigma_{l,eff} = {\varepsilon_l}^{1.5} \sigma_l, \sigma_{s,eff} = {\varepsilon_{1.5}}^{1.5} \sigma_s \tag{3.11}$$

$$i_{v,total} = \sum_m i_{v,m} + i_{v,dl} \tag{3.12}$$

This boundary condition has two subheadings entitled Particle Intercalation and Porous Electrode Reaction. In the first part, the parameters required for the mass transfer process between the porous spaces of the spherical face electrode are given. It should be noted that Fick's law has been used to establish equations and mass transfer relations. In the Porous Electrode Reaction part, the parameters related to performing the reaction are entered. It should be noted that the kinetic expression of the chemical reaction in this simulation is in the state of Lithium Insertion because this equation requires parameters that are easier to measure, and COMSOL software offers the same state in the default state for lithium-ion batteries.

3.2.1. Case study

In this case study, the discharge time of the battery in two different temperatures in a Lithium-ion battery has been investigated. The battery discharge time is one of the most important parameters in simulating lithium-ion batteries. So, the quantity was examined in the graph of changes in battery potential over time. And in all the simulation processes, battery temperature is considered constant in all stages. In the structure of the battery, the positive electrode is considered to be $LiMn_2O_4$ and $LiPF_6$ is considered the electrolyte, and the negative electrode is considered as the form of a surface boundary condition in the geometry of the battery [27]. The 2D simulated model of a Li-ion battery with COMSOL software was with $50A/m^2$ as discharge current density.

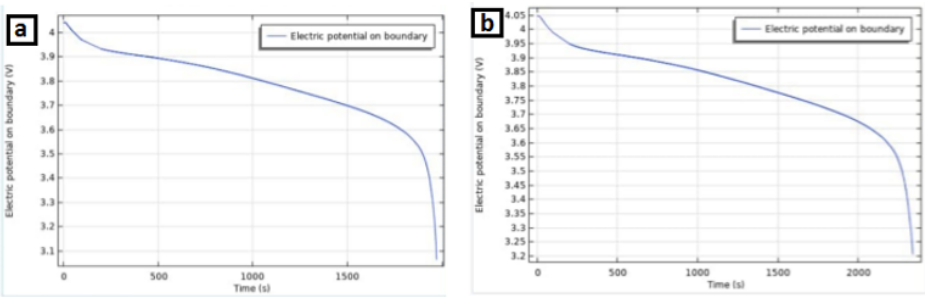

Figure 3.3: Electric potential on boundary versus Time a) at 273°K b) at 350°K [27].

As shown in Figure 3.3 , showing that temperature changes can have a direct effect on battery discharge time, so the higher the temperature, the higher the discharge time. In fact, by increasing the temperature the rate of discharge current enhances, and when the discharge current is considered constant the discharge time increases. The obtained plots demonstrated that the discharge time increases as the battery's temperature enhances. The results are related to the reduction of the resistances inside the battery as the temperature increases which can lead to better performance and higher discharge time of the battery. Also, increasing the temperature improves battery performance. But these batteries are often used in devices such as mobile phones and laptops, so the temperature cannot be considered too high because other components may be damaged. So, there is always an optimal value for the battery temperature depending on its use in devices in which the battery has the maximum efficiency.

3.2.2. Supercapacitor, electrochemical energy storage devices modeling. Temperature, and concentration distribution

3.2.3. Why supercapacitors?

Supercapacitors are electrochemical energy storage devices that can be charged in seconds to minutes and have the distinct advantage of a combination of high output power and high cycle life compared to batteries, as they can be stable for more than $100,000$ cycles. This energy-efficient storage is based on the adsorption of an electrolyte to a high surface electrode. The special properties and superiority of supercapacitors have led to extensive coordinated research on the nature of supercapacitors, storage mechanism, electrode design, and the use of new special and efficient nanomaterials in the construction of supercapacitors. In this regard, mathematical modeling and the use of specialized simulators in this field such as COMSOL and FLUENT are effective and powerful tools in the design, development, and optimization of energy storage devices. And the effect of effective parameters in design and construction, especially the effect of material type on the performance of the supercapacitor, in this modeling and simulation is examined in detail and the performance of the fabricated part can be easily predicted [38, 39].

Certainly, the type of mathematical model used to express the physics of the problem will play a key role in predicting the accuracy of the calculations performed. Farsi and Gobald [40]-[42] investigated the behavior of capacitors consisting of metal oxide nanoparticles using the Lin model et al [43]. In addition, Pech et al. [44] used simulation to investigate the effect of the geometric configuration of tangled surface micro capacitors on their performance. It seems that none of the above models can be used to predict the performance of the new asymmetric capacitor because previous models are designed for capacitors with two identical electrodes. HAO et al. 2016focused on the modeling of the asymmetric supercapacitors that represent the good future of energy storage devices because of their good performance concerning both energy density and power density [45].

They present a mathematical model for the simulation of an asymmetric supercapacitor, that structure consists of a $LiMn_2O_4$ electrode and an activated carbon (AC) electrode. Generally, the dynamic model is used to investigate the effective parameters of supercapacitor structure for the prediction of electrical, and concentration fields and the effect of the thickness of the AC electrode on supercapacitor performance in COMSOL multiphysics. A mathematical model is created to predict the performance of asymmetric capacitors. In this model, the Faraday process and the two-layer process occur at different electrodes. The falls are considered separately with a series of related settings. In the developed dynamic model, both electric field and concentration are included and nonlinear pair equations are solved by the COMSOL Multiphysics technique. Using the model, the effect of the thickness of an AC electrode on the performance of a supercapacitor has been investigated. With this simulation, the production, consumption, and transmission of lithium ions are discussed and energy densities and power densities are calculated [45]. For a proper simulation, it needs to have correct modeling of the system under study and with proper simulation, and can design different supercapacitors with different sizes, geometries, and materials and test their performance in different conditions.

3.2.4. Mathematical models in supercapacitors

For mathematical modeling of supercapacitors, some of the important material balance and electrical balance will be solved simultaneously. In this regard, model equations such as the Continuity equation for material balances of ion transfer, the faradaic process for modeling electric characteristics, the double-layer process, the porosity characteristic of the electrodes, and the ion transport along with the capacitor and inside the particles will be considered. Figure 3.4 presents a sample schematic diagram of an asymmetric supercapacitor in the typical structure that was considered to use in the modeling of a supercapacitor as a case study to be used. Which consists of two different electrodes and a separator and the faradaic redox reaction occurs in the positive electrode during charge/discharge. Mathematical modeling and several simulation methods have been developed to describe and predict the voltammetry of supercapacitor cycles. In this regard, the use of an equivalent resistance-capacitor circuit is one of the most widely used methods for tracking voltammograms, which connects the desired

number of resistors and capacitors in series or parallel. However, resistor-capacitor circuit models with shortcomings such as ion diffusion, non-uniform ion concentration in electrolytes, and electrode morphology are ignored [46].

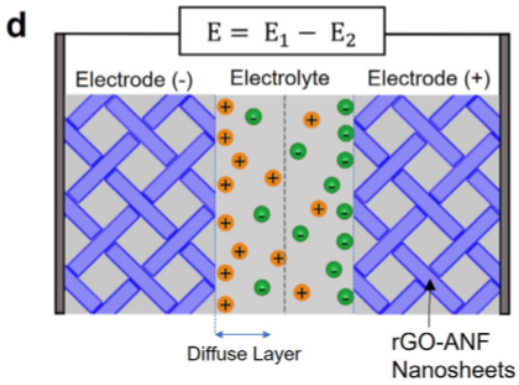

Figure 3.4: Schematic diagram of a typical rGO/ANF nanosheet in a supercapacitor [44].

Generally, the Poisson-Nernst-Planck equation (3.13) is used to calculate the ion transfer across the electrolyte. The local electric potential $E(x,t)$ in the diffuse layer for binary electrolyte solution is determined by the one-dimensional Poisson equation as [43]-[46].

$$\frac{\partial}{\partial x}\left(\in_0 \in_r \frac{\partial E}{\partial x}\right) = -F\sum_{i=1}^{2} z_i c_i \tag{3.13}$$

In this equation, z_i and $c_i(x,t)$ is the charge number of the species $i$and concentration $\left(mol/m^3\right)$, respectively. ε_0 is the vacuum permittivity and ε_r is the relative permittivity of the electrolyte solution. The ion concentration in the electrolyte diffuse layer is calculated by the Nernst-Planck equation (3.14), [46]-[49].

$$\frac{\partial c_i}{\partial t} = \nabla.\left[D_i\left(\nabla C_i + C_i\frac{z_i F}{RT}\nabla E\right)\right] \tag{3.14}$$

where Di is the diffusion coefficient, F is the Faraday's constant, R is the universal gas constant and T/K is the temperature.

On another side, the natural convection in the solution is not considered, since it is assumed that the solution is in a stagnant condition, the diffusion of the electroactive species within the thin layer and near the surface is described by Fick's second law as (3.15), [50]-[52].

$$\frac{\partial C_i}{\partial t} = D_i\frac{\partial C_i}{\partial x} \tag{3.15}$$

At the electrode-electrolyte interface, during cyclic voltammetry measurements, the potential of $E(t)$ is applied linearly with time. Both Faradaic j_F and non-Faradaic (j_c capacitive) processes can take place at an electrode-electrolyte interface. The total current density at the pseudocapacitive electrode-electrolyte interface in equation (3.16) is the sum of j_c and j_F current densities.

$$j_{total} = j_F + j_c \tag{3.16}$$

In above equation (3.16), the capacitive current density j_c is expressed in below equation (3.17) as:

$$j_c = -Cdl\partial E/\partial x, \tag{3.17}$$

The Faradaic current density j_F is expressed by the concentration-dependent Butler-Volmer equation (3.18) as below [50], [53]-[55]

$$j_f = j_0\left\{C_R\,exp\left[\alpha_a\frac{f}{RT}\eta\right] - C_0\exp\left[\alpha_c\frac{F}{RT}\eta\right]\right\} \tag{3.18}$$

Where F, α_a, α_c, j_0 are the Faraday's constant, anodic and cathodic transfer coefficients, and the exchange current density respectively. And the η is calculated by the following equation (3.19).

$$\eta = E - E_{eq} \tag{3.19}$$

The necessary boundary conditions of the model are assumed and established to solve the charge balance and ion transfer balance in the electrode structure. Usually, in using simulation software such as COMSOL it is easy to establish these boundary conditions.

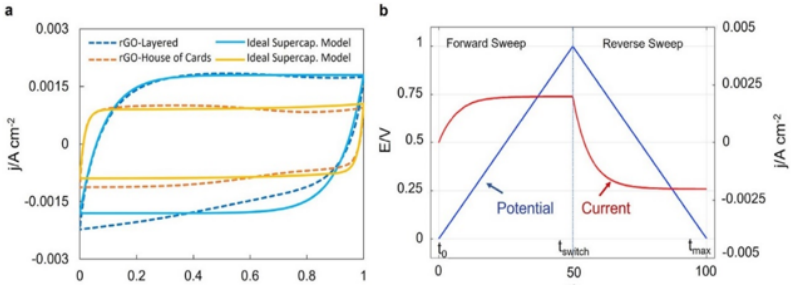

Figure 3.5: The cyclic voltammetry measurements of rGO supercapacitors nanostructures [46].

3.2.5. Case study

To use these mathematical models in supercapacitors as a case study, cyclic voltammetry of a supercapacitor was examined and the results the below [46].
In this case study, the cyclic voltammetry of rGO-ANF (reduced graphene oxide with aramid nanofiber) structural supercapacitors is simulated through COMSOL Multiphysics modeling. The result shows that during cyclic voltammetry, the reaction kinetics can be explained varying by electric potential. The simulation of cyclic voltammetry can be used to determine the more important parameters such as exchange current density, equilibrium potential, and reaction rates by comparing the predicted and measured voltammograms.

4. Conclusion

Considering that the basic principles of both energy conversion and energy storage systems are based on the properties of semiconductors and based on the electrochemical principles of electron transfer, the difference is that in the solar cell system, the principles based on electron-hole transfer and the electrical properties of semiconductors are of interest, and in the case of fuel cells, the principles based on electron-ion transfer and the electrical properties of semiconductors are of interest in these Multiphysics phenomena.

Similarly, it can be stated that the basic principles of both energy storage systems such as batteries and supercapacitors are also based on the electrochemical principles of electron and ion transfer. Therefore, the mathematical equations governing these processes are very similar and often common. Based on this review study, the common mathematical models in electrochemical devices are concluded and described below: Poisson's equation is the common equation between all electrochemical processes. Usually, reaction kinetics related to supercapacitors and fuel cells use the Butler-Volmer equation, which is a common equation in these electrochemical processes.

Also, Ohm's law for electron exchange is common in most electron transfer systems for modeling electron exchange. The relationship between charge transfer and over potential can be described using the Butler-Volmer and Tafel equations. This equation is common for most energy conversion and storage phenomena.

The Stefan- Maxwell and/or Fick's law equations are to be used to modeling of mass transfer, both bulk transfer and diffusion in porous electrodes (anode and cathode flow channels) depending on the structure and type of the energy device. The heat conduction equation is used to model heat transfer phenomena in the energy system with solid/ liquid systems. In general, the heat conduction equation is to be used in the modeling of the temperature profiles of all electrochemical devices such as solar cells, fuel cells, batteries, and supercapacitors.

Acknowledgements

The authors would like to thank the University of Sakarya and the University of Tabriz for their kind contributions.

Funding

There is no funding for this work.

Availability of data and materials

Not applicable.

Competing interests

The authors declare that the current work is derived from the M.Sc. thesis of Seyyed Reza Hosseini, which was Supervised by Prof. Dr. Aligholi Niaei and Advisor Asst. Prof. Dr. Nagihan Delibaş continued, in the Department of Chemical Engineering, University of Tabriz.

Author's contributions

All authors contributed equally to the writing of this paper. All authors read and approved the final manuscript.

References

[1] N. Delibaş, A. Moradi, S. Hosseini, M. Maleki, M. Bahramgour, A. Niaei, *Investigation of the effect of polymeric and non-polymeric materials in the hole transfer layer on the performance of perovskite solar cell*, KSU J. Eng. Sci., **25**(1) (2022), 1–6.

[2] S. Hosseini, M. Bahramgour, N. Delibaş, A. Niaei, *Interface Modification by Using an Ultrathin P3HT Layer in a Custom Perovskite Solar Cell Through SCAPS-1D Simulation,* SAU J. Sci., **25**(5) (2021), 1168–1179.

[3] M. Burgelman, K. Decock, A. Niemegeers, J. Verschraegen, S. Degrave, *SCAPS Manual*, February, 2016.

[4] J. Nelson, *The physics of solar cells,* Imperial College Press, 2003.

[5] A. Hinsch, S. Behrens, M. Berginc, H. Bönnemann, H. Brandt, A. Drewitz, *Material development for dye solar modules: results from an integrated approach,* Prog Photovolt: Res. Appl., **16**(6) (2008), 489–501.

[6] S. Wenger, M. Schmid, G. Rothenberger, A. Gentsch, M. Gratzel, J. O. Schumacher, *Coupled optical and electronic modeling of dye-sensitized solar cells for steady-state parameter extraction*, J. Phys. Chem. C, **115**(20) (2011), 10218-10229.

[7] S. Schöche, N. Hong, M. Khorasaninejad, A. Ambrosio, E. Orabona, P. Maddalena, F. Capasso, *Optical properties of graphene oxide and reduced graphene oxide determined by spectroscopic ellipsometry,* Appl. Surf. Sci., **421**, (2017), 778-782.

[8] J. M. Ball, S. D. Stranks, M. T. Hörantner, S. Hüttner, W. Zhang, E. J. W. Crossland, I. Ramirez, M. Riede, M. B. Johnston, R. H. Friend, H. J. Snaith, *Optical properties and limiting photocurrent of thin-film perovskite solar cells*, Energy Environ. Sci., **8**(2) (2015), 602-609.

[9] P. Pattanasattayavong, G. O. Ndjawa, K. Zhao, K. W. Chou, N. Gross, B. C. Regan, A. Amassian, T. D. Anthopoulos, *Electric field-induced hole transport in copper (I) thiocyanate (CuSCN) thin-films processed from solution at room temperature*, ChemComm, **49**(39), (2013), 4154-4156.

[10] T. H. Anderson, M. Faryad, T. G. Mackay, A. Lakhtakia, R. Singh, *Combined optical–electrical finite-element simulations of thin-film solar cells with homogeneous and nonhomogeneous intrinsic layers*, J. Photonics Energy, **6**(2), (2016), 025502.

[11] S. Hosseini, N. Delibaş, M. Bahramgour, A. T. Mashayekh, A. Niaei, *Performance Comparison of Different Hole Transport Layer Configurations in a Perovskite-based Solar Cell using SCAPS-1D Simulation*, Eur J Sci Technol, (31), (2021), 121–126.

[12] A. Bouarissa, A. Gueddim, N. Bouarissa, H. M. Meherezi, *Modeling of ZnO/MoS2/CZTS photovoltaic solar cell through window, buffer and absorber layers optimization*, Mater. Sci. Eng., B, **263** (2021), 114816.

[13] A. M. Islam, S. Islam, K. Sobayel, E. Emon, F. A. Jhuma, M. Shahiduzzaman, M. J. Rashid, *Performance analysis of tungsten disulfide (WS2) as an alternative buffer layer for CdTe solar cell through numerical modeling,* Opt Mater, **120** (2021), 111296.

[14] E.Y. Plotnikova, A.V. Arsentiev, M. E. Harchenko, *Textured solar cell modeling in TCAD*. In IOP Conf. Series, Mater Sci Eng, **1035**(1), (2021), 012002.

[15] M. Rasheed, M. N. A. Darraji, S. Shihab, A. Rashid, T. Rashid, *The numerical Calculations of Single-Diode Solar Cell Modeling Parameters*, Int J of Phys: Conf. Series **1963**(1) (2021), 012058.

[16] P. Saxena, N. E. Gorji, COMSOL *simulation of heat distribution in perovskite solar cells: coupled optical–electrical–thermal 3-D analysis,* IEEE J Photovoltaics, **9**(6), (2019), 1693-1698.

[17] N. Delibaş, S. Bahrami Gharamaleki, M. Mansouri, A. Niaei, *Reduction of operation temperature in SOFCs utilizing perovskites: Review,* Int. Adv. Res. Eng., **06**(1), (2022), 56-67.

[18] M. Ahangari, *Investigation of Current, Temperature, and Concentration distribution of a Solid Oxide Fuel Cell with Mathematical Modelling Approach*, M.Sc. Thesis, The University of Tabriz, 2021.

[19] S. Hussain, L. Yangping, *Review of solid oxide fuel cell materials: Cathode, anode, and electrolyte*, Energy Transitions, **4**(2) (2020), 113–126.

[20] M.Z. Ahmad, S.H. Ahmad, R.S. Chen, A.F. Ismail, R. Hazan, N. A. Baharuddin, *Review on recent advancement in cathode material for lower and intermediate temperature solid oxide fuel cells application,* Int J Hydrog Energy, **47**(2) (2022), 1103–1120.

[21] T. B. Ferriday, P. H. Middleton, *Alkaline fuel cell technology-A review*, Int. J. Hydrog. Energy, **46**(35) (2021), 18489-18510.

[22] A. M. Abdalla, S. Hossain, A. T. Azad, P. M. I Petra, F. Begum, S. G. Eriksson, A. K. Azad, *Nanomaterials for solid oxide fuel cells: A review,* Renew. Sust. Energ Rev., **82**(1), (2018), 353-368.

[23] N. Kurahashi, K. Murase, M. Santander, *High-Energy Extragalactic Neutrino Astrophysics*, Annu. Rev. Nucl. Part Sci., **72**, 2022.

[24] N. Shaari, S. K. Kamarudin, R. Bahru, S. H. Osman, N. A. Ishak, *Progress and challenges: Review for direct liquid fuel cell*, Int. J. of Energy Research, **45**(5), (2021), 6644-6688.

[25] L. Shu, J. Sunarso, S. S. Hashim, J. Mao, W. Zhou, F. Liang, *Advanced perovskite anodes for solid oxide fuel cells*: A review, Int. J. Hydrog. Energy, **44**(59) (2019), 31275–31304.

[26] M. Singh, D. Zappa, E. Comini, *Solid oxide fuel cell: Decade of progress, future perspectives and challenges*, Int. J. Hydrog. Energy, **46**(54) (2021), 27643-27674.

[27] M. Kooshki, N. Delibaş, S. Bahrami, A. Niaei, *2D Modeling of Lithium-Ion Battery Using COMSOL Multiphysics,* 4th Int. Cong. on Eng Sci Multidiscip Appro, İstanbul, 03-04 Nov. (2022), 603–608.

[28] M. A. Gabalawy, N. S. Hosny, S. A. Hussien, *Lithium-Ion Battery Modeling Including Degradation Based on Single-Particle Approximations,* Batteries **6**(3) (2020), 37.

[29] Z. Feng, W. Peng, Z. Wang, H. Guo, X. Li, G. Yan, J. Wang, *Review of silicon-based alloys for lithium-ion battery anodes*, Int. J. Mineral Metall. Mater., **28**(10) (2021), 1549-1564.

[30] H. Zhang, M. Zhou, C. Lina, B. K. Zhu, *Progress in polymeric separators for lithium ion batteries,* RSC Adv, **5**(109) (2015), 89848–89860.

[31] Y. Miao, P. Hynan, A. Jouanne, A. Yokochi, *Current Li-ion battery technologies in electric vehicles and opportunities for advancements,* Energies, **12**(6) (2019), 1074.

[32] N. Nitta, F. Wu, J. T. Lee, G. Yushin, *Li-ion battery materials: present and future,* Mater Today, **18**(5) (2015) 252–264.

[33] Y. Li, Z. Zhou, W. T. Wu, *Three-dimensional thermal modeling of Li-ion battery cell and 50 V Li-ion battery pack cooled by mini-channel cold plate,* Appl. Therm. Eng., **147** (2019), 829–840.

[34] V. R. Subramanian, V. Boovaragavan, V. D. Diwakar, *Toward real-time simulation of physics based lithium-ion battery models*, Electrochem. Solid-State Lett., **10**(11) (2007), A255.

[35] L. Cai, R. E. White, *Mathematical modeling of a lithium ion battery with thermal effects in COMSOL Inc. Multiphysics (MP) software*, J. Power Sources, **196**(14) (2011), 5985-5989.

[36] D. H. Jeon, S. M. Baek, *Thermal modeling of cylindrical lithium ion battery during discharge cycle,* Energy Convers. Manag. **52**(8-9), (2011), 2973–2981.

[37] A. Lavacchi, U. Bardi, C. Borri, S. Caporali, A. Fossati, I. Perissi, *Cyclic voltammetry simulation at microelectrode arrays with COMSOL Multiphysics*, J. Appl. Electrochem., **39** (2009) 2159–2163.

[38] K. Krois, L. Hüfner, J. Gläsel, B. J. M. Etzold, *Simulative approach for linking electrode and electrolyte properties to supercapacitor performance,* Chemie Ingenieur Technik, **91**(6) (2019), 889–899.

[39] P. Chinnasa, W. Ponhan, W. Choawunklang, *Modeling and simulation of a LaCoO3 Nanofibers/CNT electrode for supercapacitor application,* in J Phys: Conference Series, **1380** (2019), 012101.

[40] H. Farsi, F. Gobal, *Theoretical analysis of the performance of a model supercapacitor consisting of metal oxide nano-particles*, J. Solid State Electrochem., **11**(8) (2007), 1085–1092.

[41] H. Farsi, F. Gobal, *A mathematical model of nanoparticulate mixed oxide pseudocapacitors; part I: model description and particle size effects,* J. Solid State Electrochem., **13**(3) (2009), 433–443.

[42] H. Farsi, F. Gobal, *A mathematical model of nanoparticulate mixed oxide pseudocapacitors; part II: the effects of intrinsic factors,* J. Solid State Electrochem., **15**(1) (2011), 115–123.

[43] C. Lin, J. A. Ritter, B. N. Popov, R. E. White,*A Mathematical Model of an Electrochemical Capacitor with Double Layer and Faradaic Processes*, J. Electrochem. Soc, **146**(9) (1999), 3168.

[44] Pech, D., et al., *Influence of the configuration in planar interdigitated electrochemical micro-capacitors,* J. Power Sources, **230**(2013), 230–235.

[45] D. Pech, M. Brunet, T. M. Dinh, K. Armstrong, J. Gaudet, D. Guay, *Modeling and simulation of a lithium manganese oxide/activated carbon asymmetric supercapacitor,* J. Electron Mater., **45**(1) (2016), 515–526.

[46] S. Aderyani, P. Flouda, S. A. Shah, M. J. Green, J. L. Lutkenhaus, H. Ardebili, *Simulation of cyclic voltammetry in structural supercapacitors with pseudocapacitance behavior,* Electrochim. Acta, **390** (2021), 138822.

[47] C. Lian, D. Jiang, H. Liu, J. Wu, *A generic model for electric double layers in porous electrodes*, J. Phys. Chem. C, **120** (2016), 8704–8710.

[48] M. Kroupa, G. Offer, J. Kosek, *Modeling of supercapacitors: factors influencing performance,* J. Electmchem. Soc, **163**(2016), A2475–A2487.

[49] H. Girard, H. Wang, A. d'Entremont, L. Pilon, *Physical interpretation of cyclic voltammetry for hybrid pseudocapacitors*, J. Phys. Chem. C, **119** (2015), 11349–11361.
[50] H. Wang, L. Pilon, *Accurate simulations of electric double layer capacitance of ultramicroelectrodes,* J. Phys. Chem. C, **115** (2011) 16711–16719.
[51] H. Wang, L. Pilon, *Physical interpretation of cyclic voltammetry for measuring electric double layer capacitances,* Electrochim. Acta, **64** (2012) 130–139.
[52] H. Wang, A. Thiele, L. Pilon, *Simulations of cyclic voltammetry for electric double layers in asymmetric electrolytes: a generalized modified Poisson-Nernst-Planck model,* J. Phys. Chem. C, 117, (2013), 18286–18297. M. Bohner, A. Peterson, (Eds.), Advances in Dynamic Equations on Time Scales, Birkhäuser, Boston, 2003.
[53] A. Bard, L. Faulker, *Electrochemical Methods, Fundamentals and Applications*, Wiley and Sons, New Jersey, (2001), 137–153.
[54] T. Fuller, J. Harb, *Electrochemical Engineering*, Wiley Sons, New Jersey, (2018), 41–87.
[55] J. Newman, K. T. Alyea, *Electrochemical Systems,* Wiley Sons, New Jersey, (2004), 269–315.